

# Heparinized nanohydroxyapatite/collagen granules for controlled release of vancomycin

Catarina C. Coelho, Susana R. Sousa, Fernando J. Monteiro

**Abstract:** The purpose of this study was to develop a bone substitute material capable of preventing or treating osteomyelitis through a sustainable release of vancomycin and simultaneously inducing bone regeneration. Porous heparinized nanohydroxyapatite (nanoHA)/collagen granules were characterized using scanning electron microscopy, micro-computed tomography and attenuated total reflectance Fourier transform infrared spectroscopy. After vancomycin adsorption onto the granules, its releasing profile was studied by UV molecular absorption spectroscopy. The heparinized granules presented a more sustainable release over time, in comparison with nonheparinized nanoHA and nanoHA/collagen granules. Vancomycin was released for 360 h and proved to be bioactive until 216 h. *Staphylococcus aureus* adhesion was higher on granules containing collagen, guiding the bacteria to the material with antibiotic, improving

their eradication. Moreover, cytotoxicity of the released vancomycin was assessed using osteoblast cultures, and after 14 days of culture in the presence of vancomycin, cells were able to remain viable, increasing their metabolic activity and colonizing the granules, as observed by scanning electron microscopy and confocal laser scanning microscopy. These findings suggest that heparinized nanoHA/collagen granules are a promising material to improve the treatment of osteomyelitis, as they are capable of releasing vancomycin, eliminating the bacteria, and presented morphological and chemical characteristics to induce bone regeneration.

**Key Words:** osteomyelitis, vancomycin, nanohydroxyapatite, collagen, heparin

## INTRODUCTION

Osteomyelitis is an infection of bone caused by microorganisms, and the evolution of the infection may cause bone necrosis.<sup>1</sup> *Staphylococcus aureus* is the most frequently involved pathogen in this infection.<sup>1,2</sup> Despite the improvements in the treatment of osteomyelitis, it is still very difficult for orthopedic surgeons to control this infection, particularly when it is caused by resistant strains of *S. aureus*.<sup>3</sup> The prosthetic devices are very susceptible to infections that are caused mainly by *S. aureus* or coagulase-negative staphylococci (e.g., *S. epidermidis*).<sup>4</sup> In a significant number of cases, the prosthesis must be removed and replaced by another, which implies a significant impact in terms of morbidity, mortality, patient discomfort, and medical costs.<sup>5</sup> The recom-

mended treatment for osteomyelitis caused by *S. aureus* is the long-term parenteral administration of penicillin or vancomycin. In addition, the parenteral administration for this treatment involves the use of catheters, which have their own infection-associated risks and problems.<sup>1</sup> Vancomycin is a glycopeptide antibiotic with a molecular weight of approximately 1450 Da,<sup>6</sup> and it is very effective against Gram-positive bacteria, namely *S. aureus*.<sup>7</sup> In fact, this antibiotic is also capable of eradicating methicillin-resistant *S. aureus* types in opposition to penicillin. Moreover, vancomycin revealed low cytotoxicity for human osteoblasts, which is essential for bone applications.<sup>8</sup>

Nanohydroxyapatite (nanoHA) is a calcium phosphate material that is similar to natural apatite present in bone

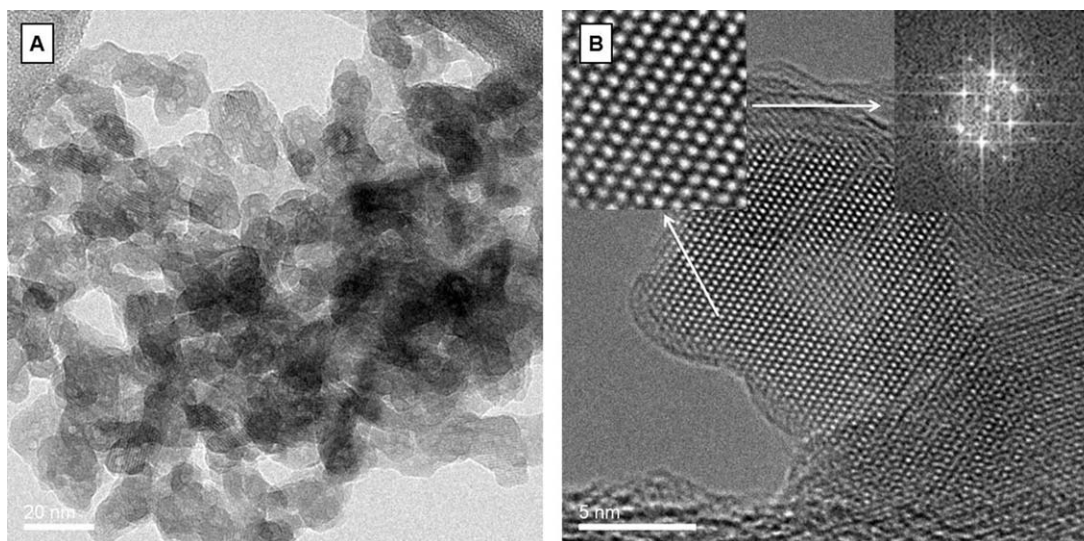


**FIGURE 1.** High-resolution transmission electron microscopy images of the nanoHA spray-dried powder. A: Nanosized HA aggregates. B: Nanocrystalline structure, evidencing the Ca atoms in a perfect crystalline lattice. Image courtesy of Prof. Paulo J. Ferreira, Material Science and Engineering Program, University of Texas at Austin and Fluidinova SA.

matrix as nanocrystals. When compared with micro-sized HA, nanoHA shows improved performance, because of large surface-to-volume ratio and higher surface reactivity.<sup>9</sup> In fact, nanoHA has properties that can control protein adsorption such as grain size, pore size, and wettability.<sup>10</sup> Moreover, nanoHA also enhances osteoblast functions like cell proliferation, calcium-containing mineral deposition, and alkaline phosphatase synthesis. NanoHA has already been studied as a potential material for drug-delivery systems, namely with vancomycin.<sup>3,11</sup> Among the numerous forms of HA available for clinical applications, porous granules are more advantageous in cases of bone defects or hollows of irregular shapes,<sup>9</sup> as it happens in patients with osteomyelitis.<sup>1</sup>

Type I collagen is a natural polymer present in bone<sup>12</sup> that has been increasingly used in tissue engineering and repair.<sup>12–14</sup> This polymer has already been tested for the improvement of mechanical and biological properties of HA. The combination of the two materials described above is probably the most direct approach to obtain a bioactive artificial material that resembles natural bone, in terms of composition, nanostructure, and biological response.<sup>15</sup>

Heparin is a glycosaminoglycan present in the extracellular matrix of different tissues<sup>16</sup> and known to interact with several relevant biomolecules, such as growth factors and collagen.<sup>17,18</sup> Therefore, immobilizing heparin on biomaterials may improve the performance of a drug-delivery system, creating sustainable releasing conditions. This glycosaminoglycan was already immobilized in a HA/collagen scaffold and proved to be a successful delivery system for bone morphogenic protein-2.<sup>18</sup>

This study aims at immobilizing heparin on nanoHA/collagen granules to allow a controlled release of antibiotic to bone, filling a debrided and previously infected bone site. For that purpose, vancomycin was adsorbed onto nanoHA/collagen granules, and its release profile was assessed, as

well as its bioactivity against *S. aureus*. Moreover, *S. aureus* adhesion to the produced granules was monitored, along with the viability of MC3T3-E1 osteoblasts cultured on granules and in the presence of vancomycin.

## MATERIALS AND METHODS

### Production of nanoHA granules

NanoHA granules were obtained by crushing sintered scaffolds and at the end passing them in sieves with pore size between 1.18 and 1.70 mm, obtaining granules with a granulometry between those two values. Scaffolds were prepared using polyurethane sponge impregnation method described elsewhere.<sup>9</sup> Briefly, polyurethane sponges (Recticel, Belgium) were impregnated with nanoHA slurry.<sup>9</sup> The slurry was prepared using a ratio of 5:4.4:0.2, respectively, of nanoHA powder (g), ultrapure water (mL), and dispersive agent Dolapix CE64 (mL) (Zschimmer & Schwarz, Germany). The nanoHA is a highly pure spray-dried powder with an average particle size of  $5.0 \pm 1.0 \mu\text{m}$ , nanoXIM-HAp202 (Fluidinova SA, Portugal), being composed by highly crystalline nanoparticles aggregates, as confirmed by high-resolution transmission electron microscopy (Fig. 1). The impregnated sponges were dried at 37 °C in the oven for approximately 30 min and then heat-treated in a sintering furnace (Thermolab). The heat treatment cycle used was as follows: heating rate of 1 °C/min till 600 °C with 1 h plateau, followed by a heating rate of 4 °C/min till 830 °C with 1 h plateau.<sup>19</sup> Afterward, the samples were naturally cooled inside the furnace.

### Collagen inclusion, crosslinking within nanoHA granules, and heparin immobilization.

A 0.5% (w/v) collagen solution was prepared by dissolving type I collagen (bovine Achilles tendon, Sigma-Aldrich, St. Louis, MO) overnight in HCl (0.01 M, pH = 2) at 4 °C. The solution was then homogenized for 3 h using an Ultra Turrax (T25 D, IKA®) at

10,000 rpm on ice and then diluted to a 0.05% solution. The nanoHA granules were spread on petri dishes, and a single drop of collagen solution was applied in each granule. Finally, the nanoHA granules were placed in a vacuum oven (Binder, Germany) at room temperature (RT, 25 °C) for 48 h to allow collagen to penetrate the granules.

Collagen chemical crosslinking was performed using *N*-(3-dimethylaminopropyl)-*N'*-ethylcarbodiimide (Aldrich, St. Louis, MO) and *N*-hydroxysuccinimide (Fluka) described elsewhere.<sup>18</sup> Briefly, 27.6 mg of *N*-(3-dimethylaminopropyl)-*N'*-ethylcarbodiimide and 10 mg of *N*-hydroxysuccinimide were dissolved on 12 mL of 2-morpholinoethane sulfonic acid buffer (0.05 M, pH = 5.4, Sigma, St. Louis, MO). The reaction was carried out for 2 h at 4 °C. After the crosslinking reaction, the solution was removed, and the samples were washed three times with 2-morpholinoethane sulfonic acid buffer and dried overnight in a vacuum oven. Considering heparinized nanoHA/collagen granules, the collagen crosslinking and heparin immobilization were performed as described earlier, with the addition of heparin, along with immobilization stoppage using phosphate-buffered saline (PBS) and a washing procedure with NaCl and ultrapure water.

#### Granules characterization

**Scanning electron microscopy.** Granules morphology, collagen distribution, and chemical characterization were studied using scanning electron microscopy (SEM) and energy-dispersive X-ray spectroscopy (FEI Quanta 400 FEG SEM/EDAX genesis X4M) with an acceleration voltage of 15 kV. Previously, the samples were fixed with Araldite on the aluminum sample holder and sputter coated with an Au/Pd alloy thin film for 90–110 s (SPI Module Sputter Coater) to yield them electrical conductivity.

**X-ray micro-computed tomography.** Three-dimensional (3D) structure of nanoHA and nanoHA/collagen granules were assessed with X-ray micro-computed tomography (micro-CT) Skyscan 1072 scanner (SkyScan, Kontich, Belgium) in high-resolution mode of 6.69  $\mu\text{m}$  x/y/z. Granules were scanned for approximately 1 h each using a pixel size of 3.29  $\mu\text{m}$ . The energy and current of the X-ray source was 57 kV and 175  $\mu\text{A}$ , respectively. A total of 250 slice images (two-dimensional) were considered and converted into binary images using a lower gray threshold of 60 and an upper gray threshold of 255, in order to distinguish ceramic material from pore voids. The slice images were assembled to yield 3D images and reveal quantitative morphological parameters. For two-dimensional and 3D image processing and visualization, two SkyScan softwares were used: CT Analyzer v.1.12.0.0 to obtain the morphological data and CTVox to create the 3D models of the granules.

**Attenuated total reflectance Fourier transform infrared spectroscopy.** The chemical composition of nanoHA, nanoHA/collagen, and heparinized nanoHA/collagen granules and crosslinked collagen was assessed with attenuated total reflectance Fourier transform infrared spectroscopy

(ATR-FTIR). For that purpose, an FTIR spectrometer (Perkin Elmer 2000, Perkin Elmer, Waltham, MA) was used, with a resolution of 4  $\text{cm}^{-1}$  and a frequency region from 400 to 4000  $\text{cm}^{-1}$ , and 100 scans were accumulated per sample. To perform ATR-FTIR, a Split Pea accessory (Harrick Scientific, Pleasantville, NY) was used containing a silicon hemispherical crystal.

#### Vancomycin release kinetics from granules

Vancomycin loading was performed by immersing 20 mg of granules in Eppendorf tubes and in 1 mL of vancomycin solution (Vancomicina Combino Pharm) with a concentration of 25 mg/mL (pH = 4). The antibiotic adsorption onto granules was performed at 37 °C and 120 rpm in the orbital shaker (KS 4000 IC, IKA®) for 24 h.

After loading, the supernatant solution was removed, and the granules were transferred to new Eppendorf tubes, and 1 mL of PBS (pH = 7.4) was added. Eppendorf tubes were placed in the orbital shaker at 37 °C and 120 rpm. To determine the vancomycin release from the granules, 200  $\mu\text{L}$  of solution was withdrawn and replaced by fresh PBS solution after 0.25, 0.5, 1.5, 2.5, 3.5, and 24 h and from then onward every 24 h up to 360 h. Control experiments using antibiotic-free ceramic samples was performed under the same experimental conditions (negative control). The removed solution was centrifuged for 5 min and 14,000 rpm to avoid particles in suspension. Vancomycin concentration was determined by molecular absorption spectroscopy at 280 nm using a spectrophotometer (Lambda 35 UV/Vis Spectrometer, Perkin Elmer). The collected samples were subsequently frozen at  $-20$  °C to perform microbiology assays. All tests were performed in triplicate.

#### Vancomycin bioactivity

Vancomycin bioactivity was assessed using broth microdilution method.<sup>20</sup> Therefore, *S. aureus* ATCC 25923 was grown on nutrient broth (Liofilchem, Italy) for 24 h at 37 °C and 120 rpm. From that bacterial suspension, an inoculum was taken and adjusted to an absorbance (640 nm) of 0.2, corresponding to  $3.8 \times 10^8$  colony forming units (CFU)/mL. Afterward, 96-well plates were filled with bacterial suspension (180  $\mu\text{L}$ ) and with the released vancomycin (20  $\mu\text{L}$ ). For each time point, eight wells were used. Nutrient broth without bacteria and bacterial suspension without vancomycin were established as controls. The plates were incubated for 24 h at 37 °C and 120 rpm. After incubation, the absorbance was measured at 640 nm using a microplate reader (Spectramax M2e, Molecular Devices, Sunnyvale, CA). The absorbance values were converted to total number of bacteria/mL using a calibration curve.

#### *S. aureus* adhesion to granules

**Quantification of adherent *S. aureus*.** The adherence of *S. aureus* on three type of granules was studied to see whether the bacterium has some tendency to migrate to one type of granules rather than to another. With that objective, a nutrient agar (Liofilchem, Italy) plate inoculated with

*S. aureus* ATCC 25923 was used to create a  $1.5 \times 10^8$  CFU/mL suspension in 0.9% NaCl, which equals to 0.5 McFarland equivalence turbidity standard in ambient light, using a densitometer (BioMerieux, France). To allow bacterial adhesion to granules, 20 mg of granules were placed in a glass tube with 1 mL of bacterial suspension and incubated in a gently shaking water bath at 37 °C for 1 h. The experiment was performed in triplicate. After incubation, each sample was washed twice with 0.9% NaCl to remove loosely adhered or nonadherent bacteria. Then, 5 mL of 0.9% NaCl was added to each tube and sonicated for 1 s at 20 kHz using a sonicator (Sonoplus HD 2200, Bandelin, Germany) with a MS 73 probe. The sonicated solutions were used to obtain serial dilutions, and these were placed onto nutrient agar culture plates and incubated at 37 °C for 18 h. Afterward, the number of adherent bacteria was counted, and the number of CFU/mm<sup>2</sup> was determined.

**Adherent *S. aureus* imaging.** *S. aureus* was fixed using 1.5% glutaraldehyde in cacodylate buffer (0.14 M) for 10 min and dehydrated in graded series of ethanol solutions. The samples were dried overnight at RT. Adherent *S. aureus* on granules were visualized using SEM as previously described.

#### Osteoblast culture

MC3T3-E1 cells, an osteoblastic cell line derived from mouse calvaria, were grown in alpha minimum essential medium (Gibco, Life Technologies, Grand Island, NY), supplemented with 1% penicillin-streptomycin (Gibco) and 10% fetal bovine serum (Invitrogen, Carlsbad, CA). Cells were incubated in a humidified environment at 37 °C and 5% of CO<sub>2</sub>. Vancomycin adsorption on granules was performed as mentioned earlier. Granules were placed in 96-well plates, and cells were seeded using a density of  $5 \times 10^4$  cells/mL. Cells were cultured for 21 days, and medium was changed three times a week. As control, cells were cultured on tissue culture polystyrene (TCPS) with the same conditions used for the granules. For each condition, six replicates were used for the resazurin assay.

**Metabolic activity.** The nontoxic alamar blue (resazurin) dye was used to determine the metabolic activity of MC3T3-E1 cells. The blue nonfluorescent dye is metabolized by cells, converting it to a reduced pink fluorescence dye.<sup>21</sup> Therefore, 10% (v/v) of resazurin was added to the medium and incubated for 4 h at 37 °C and 5% of CO<sub>2</sub>. Afterward, 100 µL was transferred into a black 96-well plate, and fluorescence was measured at 530 nm excitation and 590 nm emission wavelength with a fluorescence reader (SynergyMix, BioTek, Winooski, VT) using Gen5 1.09 Data Analysis Software. These measurements were made at 24 h and 4, 7, 14, and 21 days of culture.

**Cell morphology. Scanning electron microscopy.** Granules with seeded cells were rinsed with PBS and fixer using 1.5% glutaraldehyde (v/v) (Agar) in 0.14 M sodium cacodylate buffer (Merck, Kenilworth, NJ) at RT for 30 min. The

samples were washed twice with PBS and then dehydrated in graded series of ethanol. Hexamethyldisilazane (Sigma) was added, and the samples were dried overnight at RT. Granules were visualized on SEM as previously described.

**Confocal laser scanning microscopy.** Granules with seeded cells were fixed using 4% paraformaldehyde for 15 min and then washed twice with PBS. Triton X-100 0.1% was used, for 5 min, to permeabilize the cells, and the cells were then incubated in 1% bovine serum albumin at 37 °C for 30 min. After incubation, the staining of the F-actin filaments was performed using Alexa Fluor 594 Phalloidin (1:100, Molecular Probes A12379, Invitrogen) in 1% bovine serum albumin at RT for 20 min in dark. The samples were then washed twice with PBS. Cell nuclei were stained with a solution of Hoechst dye (1:1000, Sigma) in PBS at RT for 15 min in dark. Finally, the samples were washed twice with PBS, and one drop of Vectashield was added. The images were acquired with a Leica SP5 Confocal microscope, using a  $\times 20$  oil immersion objective. The obtained images were processed with Leica Application Suite version 2.6.0.

#### Statistical analysis

The statistical analysis was performed using one-way analysis of variance followed by a *post hoc* Tukey's test with a significance level of  $p < 0.05$ . The data analysis was done using GraphPad Software version 5.02 (GraphPad software, San Diego, CA).

## RESULTS

#### Granules characterization

Granules morphology and collagen distribution were characterized by SEM analysis. The obtained images revealed the presence of interconnective macroporosity [Fig. 2(A)]. Moreover, SEM shows that collagen is distributed heterogeneously on nanoHA granules. For example, it can form large collagen fibers across a macropore [Fig. 2(B,C)] or smaller fibers covering the nanoHA grains [Fig. 2(D,E)]. The presence of microporosity [Fig. 2(E)] and nanoporosity [Fig. 2(F)] was also evident.

Micro-CT was performed to visualize the 3D structure of the granules and to determine porosity ( $62.7 \pm 1.5\%$ ), mean pore size ( $227.3 \pm 7.2$  µm), and surface area ( $26.6 \pm 5.6$  mm<sup>2</sup>). The images obtained for the 3D structure of a nanoHA granule show its irregular morphology and interconnective macroporosity (Fig. 3).

The granules chemical composition was assessed using ATR-FTIR (Fig. 4). The spectra revealed phosphate groups at 473, 565, 600, 962, 1028, and 1088 cm<sup>-1</sup>. The bands at 630 and 3572 cm<sup>-1</sup> correspond to OH<sup>-</sup> vibrational and stretching modes, respectively. Considering the samples containing collagen, the characteristic peaks for amide I (C=O stretching at 1600–1700 cm<sup>-1</sup>), amide II (N–H deformation at 1500–1550 cm<sup>-1</sup>), and amide III (N–H deformation at 1200–1300 cm<sup>-1</sup>) were obtained. The crosslinked collagen sample has a broad band at 3200–3600 cm<sup>-1</sup>, indicating the presence of adsorbed water on the material.<sup>9</sup> For the heparinized nanoHA/collagen granules, there was no novel

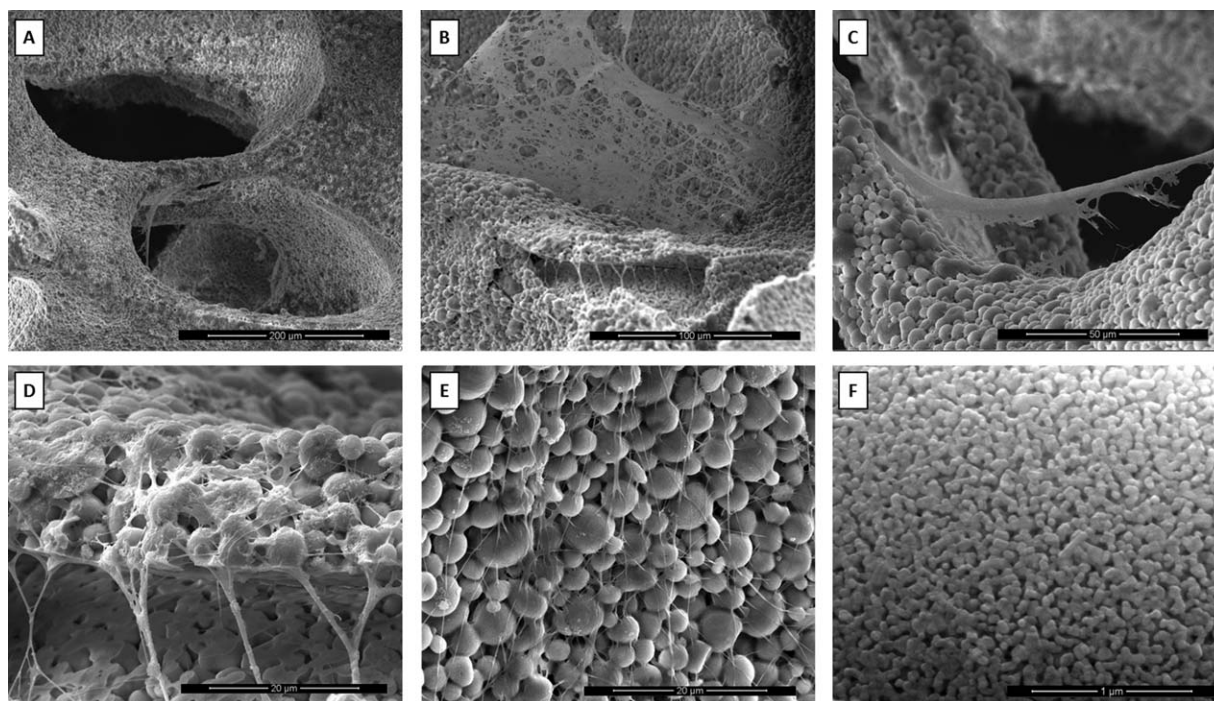


**FIGURE 2.** SEM images from nanoHA/collagen granules. A: Presence of interconnective macroporosity. B–D: Collagen distribution in a fiber-like structure on nanoHA. E: Presence of microporosity. (F) Presence of nanoporosity.

peaks present, as heparin peaks are superimposed over collagen ones.<sup>22</sup>

#### Vancomycin release kinetics from granules

The vancomycin release from granules of nanoHA, nanoHA/collagen, and heparinized nanoHA/collagen is shown in Figure 5. For the three types of granules, an initial burst of antibiotic was observed in the first 15 min. The amount of vancomycin released in the first 24 h was equal for the three types of granules. However, after 24 h, the amount of released antibiotic decreased for the nanoHA and nanoHA/collagen granules. In opposition, the heparinized granules continued a more sustainable release, with higher amounts of vancomycin present, when compared with nonheparinized granules. After 12 days, there was no antibiotic

detected for nanoHA and nanoHA collagen granules. For the heparinized granules, the vancomycin release stopped after 15 days. Considering the released concentrations detected, they were always higher than vancomycin minimum inhibitory concentration (MIC) for *S. aureus* ATCC 25923 (1 μg/mL) and below vancomycin minimum toxic concentration (50 μg/mL) for the three types of granules.

#### Vancomycin bioactivity

As heparinized granules presented the best release profile, the antibiotic bioactivity was assessed. The results show that the released antibiotic was able to inhibit *S. aureus* growth for 216 h (9 days) (Fig. 6). After that time point, bacterial growth was observed in some replicates [Fig. 6(B)], and after 288 h, bacteria grew in all replicates. Figure

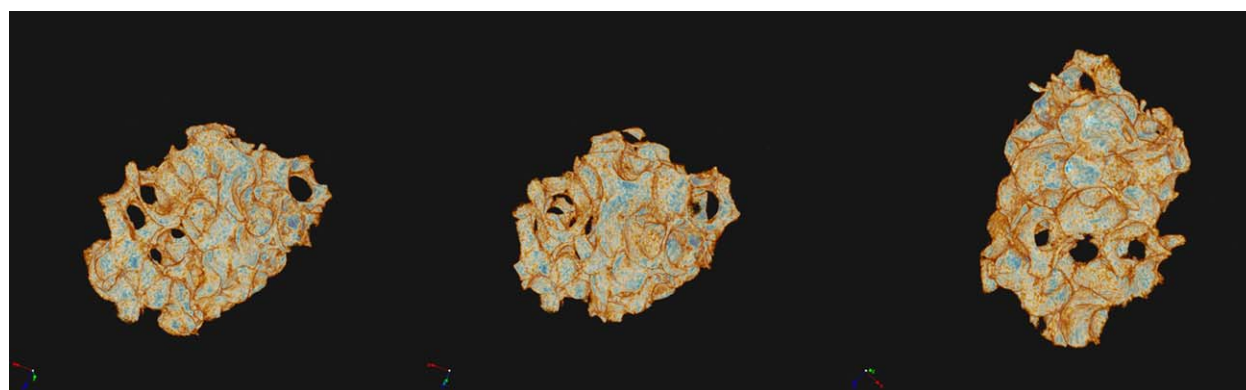


**FIGURE 3.** 3D micro-CT images from a nanoHA/collagen granule from different perspectives, showing interconnective macroporosity throughout all the granules structure. [Color figure can be viewed in the online issue, which is available at [wileyonlinelibrary.com](http://wileyonlinelibrary.com).]

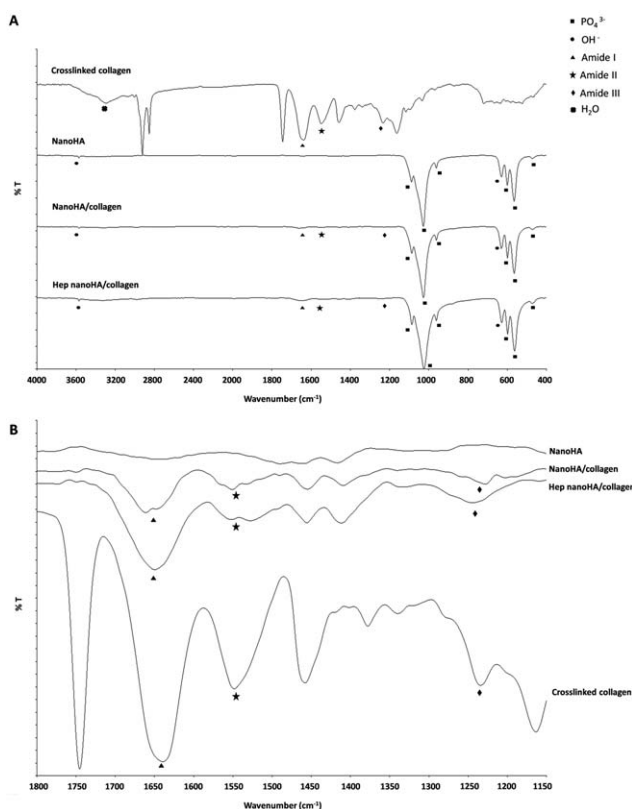


**FIGURE 4.** A: ATR-FTIR spectra of crosslinked collagen, nanoHA, nanoHA/collagen, and heparinized nanoHA/collagen granules. B: Magnification between 1150 and 1800  $\text{cm}^{-1}$  for crosslinked collagen, nanoHA, nanoHA/collagen, and heparinized nanoHA/collagen granules, indicating the respective relevant peaks.

6 indicates the concentration values of antibiotic applied in bacterial suspension. After 216 h, the concentrations were lower than the MIC, and it was expected that bacteria will

grow. If not diluted, the release concentrations would be able to inhibit bacterial growth, because they were always higher than the MIC for *S. aureus* ATCC 25923.

### *S. aureus* adhesion on granules

Figure 7 shows the results obtained for the bacterial adhesion studies. It was observed that granules containing collagen have higher number of adherent *S. aureus*, when compared with nanoHA granules [Fig. 7(A)]. SEM images of adherent bacteria on granules surface show that bacteria adhered alone or in pairs. Moreover, bacteria were frequently seen near the collagen fibers and between the nanoHA grains [Fig. 7(B)].

### MC3T3-e1 metabolic activity

In Figure 8, it is shown that there is no difference in the metabolic activity after 24 h of culture for cells with and without vancomycin. In the absence of this antibiotic, the metabolic activity of the cells increased continuously until the end of the culture. Considering the cells in the presence of vancomycin, a decrease in metabolic activity was observed until 7 days of culture. However, after 14 days of culture, it was observed that cells in the presence of vancomycin increased their metabolic activity and continued to increase it until the end of the culture (21 days).

### MC3T3-e1 morphology

SEM images (Fig. 9) show that after 24 h, cells without vancomycin are elongated and spread on the granules surface. In opposition, the cells in the presence of antibiotic did not acquire an elongated shape after 24 h. Though, after 7 days, all cells were elongated and well spread on the granules surface, as it happened with cells without antibiotic. After 14 days, an increase in cell number was

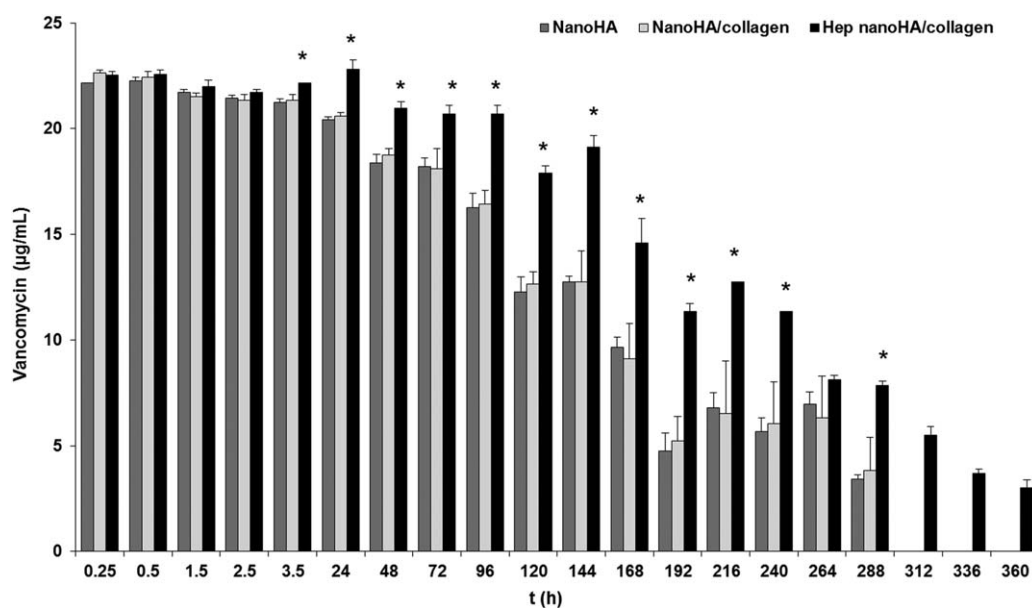
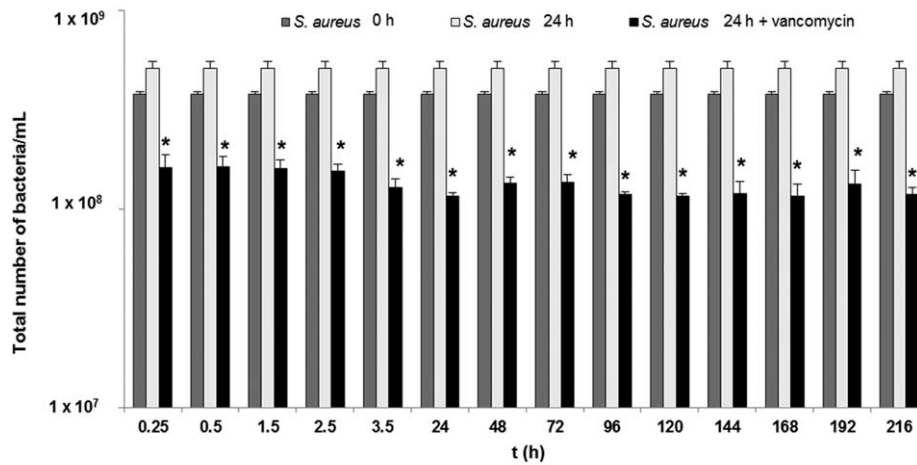


**FIGURE 5.** Vancomycin release from nanoHA, nanoHA/collagen, and heparinized nanoHA/collagen granules versus time. The values correspond to the concentration present at each time point. \*Represents a statistically significant difference compared with nanoHA and nanoHA/collagen for each time point ( $p < 0.05$ ).

A



B

	t (h)																
	0.25	0.50	1.5	2.5	3.5	24	48	72	96	120	144	168	192	216	240	264	288
Vancomycin (µg/mL)	2.254	2.258	2.198	2.170	2.217	2.281	2.096	2.069	2.069	1.791	1.911	1.457	1.133	1.272	1.133	0.814	0.786
S. aureus growth	-	-	-	-	-	-	-	-	-	-	-	-	-	-	+	++	+++

**FIGURE 6.** A: Total number of *S. aureus* in the absence of vancomycin, for 0 and 24 h of incubation, and in the presence of vancomycin after 24 h of incubation. \*Represents a statistically significant difference compared with *S. aureus* 0 h and *S. aureus* 24 h ( $p < 0.05$ ). B: *S. aureus* growth inhibition for each time point of released vancomycin. (–) No growth; (+) Growth in one replicate; (++) Growth in two replicates; (+++) Growth in five replicates.

observed for both cells with and without antibiotic, indicating that cells were proliferating. The results obtained with confocal microscopy are consistent with those from SEM. For the first time points (24 h and 4 days), it was observed that cells adhered on both granules, but the cells in the presence of vancomycin had a more rounded morphology (Fig. 9). After 7 days, it could be seen that cells in the presence of antibiotic started to elongate on the surface of the material. After 14 days of culture, both cells with and without vancomycin are well spread, covering the entire surface.

## DISCUSSION

This work proposed a novel material to be applied for the treatment of osteomyelitis. This material was prepared to allow a controlled release of vancomycin and further induce bone regeneration. The heparinized nanoHA/collagen granules were prepared and subsequent chemical and morphological characterization was carried out. The vancomycin release profile was evaluated as well as its bioactivity, *S. aureus* adhesion, and effect of released vancomycin on viability and morphology of MC3T3-E1 cells.

The produced granules presented adequate dimensions (1.18–1.70 mm) to be used in cases of chronic osteomyelitis because the defects present in this phase of infection normally are on the centimeters range in humans.<sup>23,24</sup> Moreover, the size of the granules is also adequate to perform *in vivo* studies using an osteomyelitis rat model.<sup>25</sup>

SEM images revealed the presence of interconnective macroporosity, which is desirable for bone tissue regeneration, as interconnectivity allows cell migration, neovascularization, and transport of nutrients and proteins. In addition, the presence of macroporosity induces osteoinduction.<sup>26,27</sup> Furthermore, the presence of micro [Fig. 2(E)] and nanoporosity [Fig. 2(F)] on nanoHA was evident. Microporosity is known to result in higher surface area that induces protein adsorption, ion exchange, and bone-like apatite formation.<sup>28</sup> The presence of nanoporosity also improves protein adsorption and enhances initial cell attachment<sup>29</sup> because of the large surface-to-volume ratio.<sup>9</sup>

Using micro-CT, it was only possible to assess microporosity, as the equipment does not have enough resolution to determine nanoporosity. Because the collagen fibers are transparent to X-rays, it was also impossible to detect collagen on granules. The average macroporosity of the granules is  $62.7 \pm 1.5\%$ , being adequate for bone regeneration.<sup>28</sup> The value of surface area ( $26.6 \pm 5.6 \text{ mm}^2$ ) is considered high, taking into account the granules size distribution (1.18–1.70 mm). If these particles were spherical and without pores, the geometric area would be between 4.27 and  $9.07 \text{ mm}^2$ , which is much lower than the obtained area. The average mean pore size obtained was  $227.3 \pm 7.2 \text{ µm}$ , which is adequate for osteogenesis. The minimum requirement for pore size is approximately 100 µm because of cell size and cell migration.<sup>28</sup> Moreover, previous studies from our group revealed that nanoHA granules in a co-culture system with

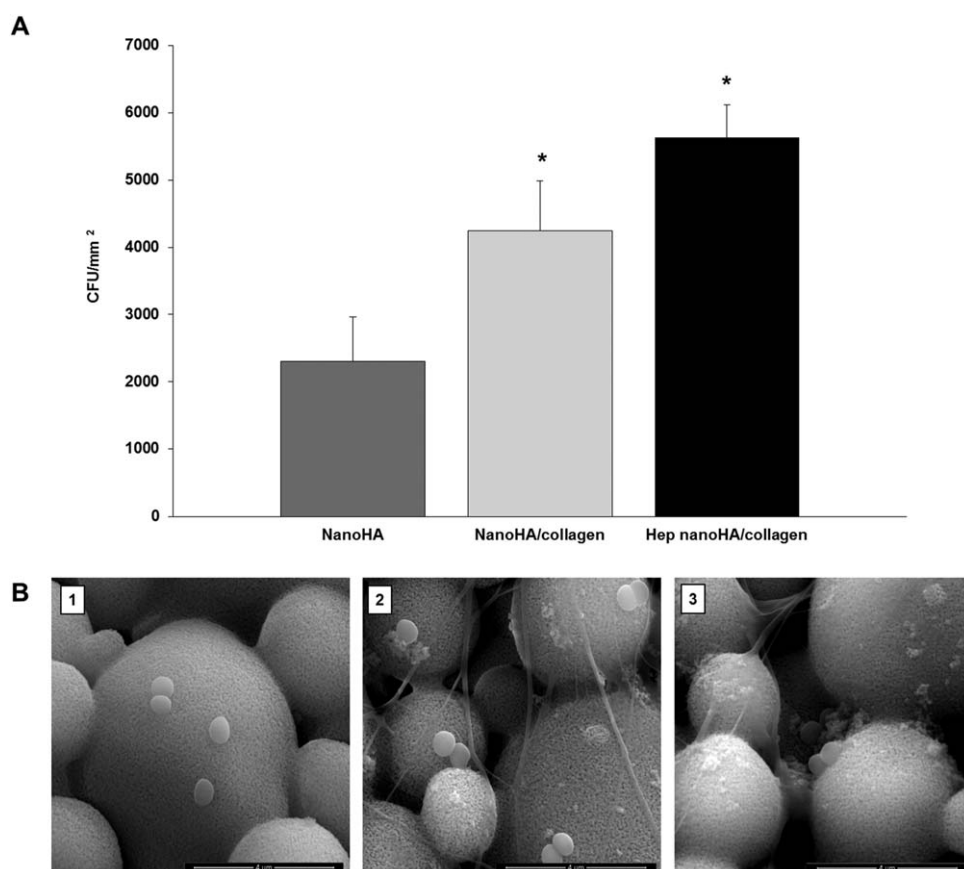


**FIGURE 7.** A: *S. aureus* adhesion onto nanoHA, nanoHA/collagen, and heparinized nanoHA/collagen granules expressed as CFU per mm<sup>2</sup> of granules. \*Represents a statistically significant difference compared with nanoHA granules ( $p < 0.05$ ); B: SEM images of adherent *S. aureus* on granules (1, nanoHA; 2, nanoHA/collagen; and 3, heparinized nanoHA/collagen).

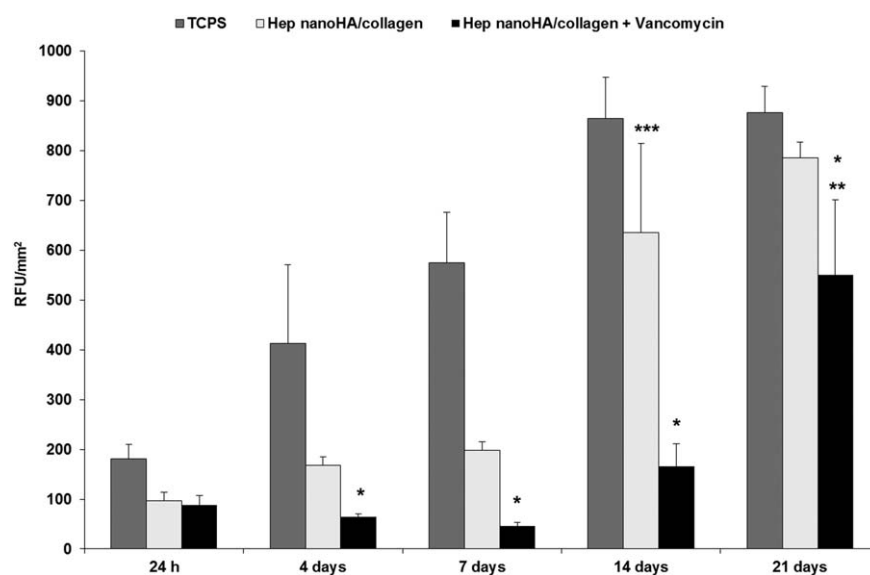


**FIGURE 8.** Metabolic activity of MC3T3-E1 cells cultured with heparinized nanoHA/collagen granules with and without vancomycin. Results are expressed in terms of relative fluorescence units (RFU) per mm<sup>2</sup> of granules. TCPS was used as a control. \*Represents a statistically significant difference compared with heparinized nanoHA/collagen granules without vancomycin for the same time point ( $p < 0.05$ ). \*\*Represents a statistically significant difference compared with heparinized nanoHA/collagen granules with vancomycin at 24 h and 4, 7, and 14 days ( $p < 0.05$ ). \*\*\*Represents a statistically significant difference compared with heparinized nanoHA/collagen granules without vancomycin at 24 h and 4 and 7 days ( $p < 0.05$ ).

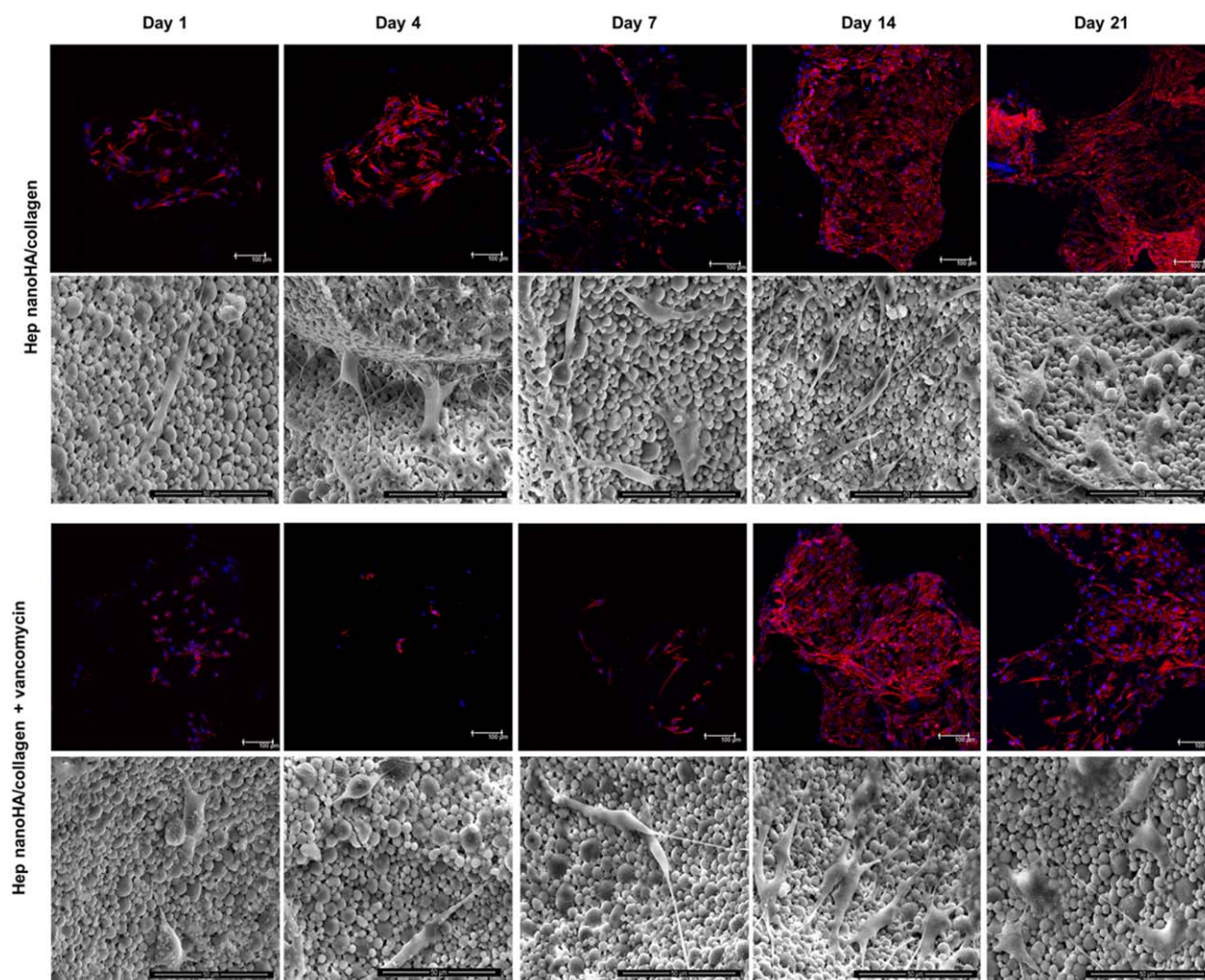


**FIGURE 9.** SEM and CLSM images of MC3T3-E1 cells morphology on heparinized nanoHA/collagen granules with and without vancomycin after 1, 4, 7, 14, and 21 days of culture. F-actin is represented in red, whereas cell nuclei were counterstained in blue with Hoechst stain. MC3 T3-E1 on TCPS was used as a control (data not shown). [Color figure can be viewed in the online issue, which is available at [wileyonlinelibrary.com](http://www.interscience.wiley.com).]

human mesenchymal stem cells and human dermal microvascular endothelial cells (HDMECs) showed positive effects in both angiogenic and osteogenic behaviors. Particularly, nanoHA granules provided appropriate environment for both human mesenchymal stem cells and HDMECs to adhere, migrate, and proliferate, maintaining their characteristic gene expression markers. Moreover, HDMECs in the presence of nanoHA granules were capable to form capillary-like tubes just after 3 days of culture.<sup>30</sup>

Considering the vancomycin release from granules, it was seen that heparinized nanoHA/collagen granules are able to release higher amounts of antibiotic in a more sustainable way, compared with nanoHA and nanoHA/collagen granules. The released vancomycin concentrations were always above *S. aureus* MIC and below minimum toxic concentration.<sup>31</sup> Therefore, the released antibiotic is enough to inhibit *S. aureus* growth without becoming toxic. Moreover, an initial burst of release was observed, followed by a sustained release. This release profile is recommended to have a complete eradication of the pathogen.<sup>5</sup> The interaction

between HA and vancomycin can be explained because HA is mostly negatively charged,<sup>32</sup> and so cationic vancomycin can adsorb onto HA. Collagen is positively charged during vancomycin adsorption (acidic pH),<sup>33</sup> being unlikely that these two molecules interact strongly as they both have the same charge.<sup>34</sup> Therefore, the similar releasing profile between these two types of granule surfaces probably is dependent on HA and the presence of nanoporosity, as vancomycin molecules can be more entrapped on the structure and consequently released slower.<sup>35</sup> The difference observed for heparinized nanoHA/collagen granules may be because heparin contains negatively charged groups (carboxylic and sulfur) and shows a tendency for protein binding.<sup>36</sup> Consequently, vancomycin has two characteristics that promote its interaction with heparin, increasing its adsorption: it is a cation and a glycopeptide. The release of vancomycin from granules can be explained by a change in the net charge of this antibiotic: as granules were placed in a solution at physiological pH (PBS solution), vancomycin net charge decreased, becoming less positive.<sup>37,38</sup> Therefore, the

interaction between vancomycin and the granules became weaker, promoting the release of antibiotic.

Regarding the vancomycin bioactivity, it was shown that the released antibiotic was able to inhibit *S. aureus* growth *in vitro* in all replicates until 216 h. In the presence of antibiotic, the total number of bacteria was lower than the number of bacteria present in the beginning of this assay. In addition, it was also observed that the bacteria were able to grow after 24 h of incubation in the absence of vancomycin. After 216 h of release, vancomycin was not capable to inhibit *S. aureus* growth in all replicates, but this was related to the concentration used on the chosen method. The latter requires a 10-fold dilution of released vancomycin concentration, therefore decreasing the actual values to figures close or below MIC [Fig. 6(B)], and leading to inhibition failure. However, a very important fact to retain is that the released concentrations were always above vancomycin MIC for *S. aureus* ATCC 25923<sup>39</sup> (Fig. 5) and, if not diluted, would be able to inhibit bacterial growth.

Considering the adhesion of *S. aureus* onto granules, a higher adhesion on granules containing collagen was detected, when compared with nanoHA granules as it was previously reported by other authors.<sup>40,41</sup> A higher adherence of *S. aureus* on granules containing collagen compared with nanoHA was also expected, because collagen is one of the extracellular matrix proteins to which *S. aureus* binds to colonize the host tissues.<sup>42,43</sup> Considering the heparinized nanoHA granules, a higher *S. aureus* adherence was expected than on nanoHA, because heparin is a glycosaminoglycan to which these bacteria can adhere in animals.<sup>16,44</sup> The higher adherence of *S. aureus* on granules may improve its eradication because the bacteria will have a tendency to migrate toward the material.

As heparinized nanoHA/collagen granules proved to be the best material for vancomycin release, the effect of this antibiotic on osteoblasts metabolic activity was studied. Therefore, a preliminary MC3T3-E1 culture experiment was performed, showing that vancomycin did not affect the cells metabolic activity for the first 24 h (Fig. 8). However, the metabolic activity decreased until day 7, compared with heparinized nanoHA/collagen granules without antibiotic. From confocal laser scanning microscopy (CLSM) and SEM studies, a reduced number of cells at days 1, 4, and 7 was also detected for the samples containing vancomycin. The low metabolic activity and cell number matches with the period during which higher amounts of vancomycin were being released from granules. Nevertheless, this result was not expected because vancomycin is considered a relatively safe and nontoxic antibiotic for osteoblasts, as reported by Rathbone et al., where a concentration of 2000 µg/mL only reduced the cell number in <25%.<sup>8</sup> However, the authors also mentioned that even if the antibiotic presented some degree of toxicity, it is important to consider whether surviving cells could remain viable and have osteogenic potential. It was observed that after 21 days of culture, the metabolic activity of MC3T3-E1 cells on granules containing vancomycin significantly increased, when compared with shorter time points. This indicates that the remaining viable

cells were able to recover and proliferate, as it was observed in CLSM and SEM images (Fig. 9). In fact, osteoblasts in the presence of vancomycin started to increase their metabolic activity and proliferate at day 14, which corresponds to the period when vancomycin release ended. Therefore, after vancomycin release, the osteoblasts that remained viable began to recover from the presence of antibiotic. The obtained results for this assay are promising because osteoblasts were able to adhere and proliferate even in the presence of vancomycin.

## CONCLUSIONS

In this work, it was possible to produce an innovative controlled releasing system aimed at improving the treatment of osteomyelitis through local antibiotic release. Porous heparinized nanoHA/collagen granules were successfully produced and exhibited interconnective macro-, micro-, and nanoporosity. This material also allowed a more sustainable and controlled release of vancomycin for 360 h (15 days), when compared with nonheparinized granules. The antibiotic released from heparinized granules was bioactive and capable of inhibiting *S. aureus* growth. The bacterial adhesion studies revealed that *S. aureus* adhere in higher number on granules containing collagen, and this behavior may improve their eradication. The presence of vancomycin did not affect the viability of MC3T3-E1 cells, as they were able to remain viable in the presence of the antibiotic and proliferate after 14 days of culture. We can envisage that the material herein developed can first eradicate osteomyelitis and then promote the renewal of bone.

## ACKNOWLEDGMENTS

The authors express their gratitude to Fluidinova S.A. (Maia, Portugal) for providing the nanohydroxyapatite powder.

## REFERENCES

1. Lew DP, Waldvogel FA. Osteomyelitis. *Lancet* 2004; 364:369–379.
2. Hatzebuehler J, Pulling T. Diagnosis and management of osteomyelitis. *Am Fam Physician* 2011; 84:1027–1033.
3. Jiang JL, Li YF, Fang TL, Zhou J, Li XL, Wang YC, Dong J. Vancomycin-loaded nano-hydroxyapatite pellets to treat MRSA-induced chronic osteomyelitis with bone defect in rabbits. *Inflamm Res* 2012; 61:207–215.
4. Landersdorfer CB, Kinzig M, Bulitta JB, Hennig FF, Holzgrabe U, Sörgel F, Gusinde J. Bone penetration of amoxicillin and clavulanic acid evaluated by population pharmacokinetics and Monte Carlo simulation. *Antimicrob Agents Chemother* 2009; 53:2569–2578.
5. Ravelingien M, Mullens S, Luyten J, D'Hondt M, Boonen J, De Spiegeleer B, Coenye T, Vervaeke C, Remon JP. Vancomycin release from poly(D,L-lactic acid) spray-coated hydroxyapatite fibers. *Eur J Pharm Biopharm* 2010; 76:366–370.
6. Rybak MJ. The pharmacokinetic and pharmacodynamic properties of vancomycin. *Clin Infect Dis* 2006; 42:S35–S39.
7. Schäfer M, Schneider TR, Sheldrick GM. Crystal structure of vancomycin. *Structure* 1996; 4:1509–1515.
8. Rathbone CR, Cross JD, Brown KV, Murray CK, Wenke JC. Effect of various concentrations of antibiotics on osteogenic cell viability and activity. *J Orthopaed Res* 2011; 29:1070–1074.
9. Laranjeira MS, Fernandes MH, Monteiro FJ. Innovative macroporous granules of nanostructured-hydroxyapatite agglomerates: Bioactivity and osteoblast-like cell behaviour. *J Biomed Mater Res Part A* 2010; 95:891–900.

10. Ribeiro N, Sousa SR, Monteiro FJ. Influence of crystallite size of nanophased hydroxyapatite on fibronectin and osteonectin adsorption and on MC3T3-e1 osteoblast adhesion and morphology. *J Colloid Interface Sci* 2010; 351:398–406.
11. Rauschmann MA, Wichelhaus TA, Stirnal V, Dingeldein E, Zichner L, Schnettler R, Alt V. Nanocrystalline hydroxyapatite and calcium sulphate as biodegradable composite carrier material for local delivery of antibiotics in bone infections. *Biomaterials* 2005; 26:2677–2684.
12. Lee CH, Singla A, Lee Y. Biomedical applications of collagen. *Int J Pharm* 2001; 221:1–22.
13. DA Wahl JC. Collagen-hydroxyapatite composites for hard tissue repair. *Eur Cells Mater* 2006; 11:43–56.
14. Cen L, Liu W, Cui L, Zhang W, Cao Y. Collagen tissue engineering: Development of novel biomaterials and applications. *Pediatr Res* 2008; 63:492–496.
15. Kikuchi M, Itoh S, Ichinose S, Shinomiya K, Tanaka J. Self-organization mechanism in a bone-like hydroxyapatite/collagen nanocomposite synthesized in vitro and its biological reaction in vivo. *Biomaterials* 2001; 22:1705–1711.
16. Ljungh Å, Moran AP, Wadström T. Interactions of bacterial adhesins with extracellular matrix and plasma proteins: Pathogenic implications and therapeutic possibilities. *FEMS Immunol Med Microbiol* 1996; 16:117–126.
17. Conrad HE. Heparin-Binding Proteins, 1st ed. Philadelphia, PA: Elsevier Science; 1997.
18. Teixeira S, Yang L, Dijkstra P, Ferraz M, Monteiro F. Heparinized hydroxyapatite/collagen three-dimensional scaffolds for tissue engineering. *J Mater Sci Mater Med* 2010; 21:2385–2392.
19. Barros J, Grenho L, Manuel CM, Ferreira C, Melo L, Nunes OC, Monteiro FJ, Ferraz MP. Influence of nanohydroxyapatite surface properties on *Staphylococcus epidermidis* biofilm formation. *J Biomater Appl* 2014; 28:1325–1335.
20. Borges A, Ferreira C, Saavedra MJ, Simões M. Antibacterial activity and mode of action of ferulic and gallic acids against pathogenic bacteria. *Microb Drug Resist* 2013; 19:256–265.
21. O'Brien J, Wilson I, Orton T, Pognan F. Investigation of the alamar blue (resazurin) fluorescent dye for the assessment of mammalian cell cytotoxicity. *Eur J Biochem* 2000; 267:5421–5426.
22. Lu Q, Zhang S, Hu K, Feng Q, Cao C, Cui F. Cytocompatibility and blood compatibility of multifunctional fibroin/collagen/heparin scaffolds. *Biomaterials* 2007; 28:2306–2313.
23. Gitelis S, Brebach GT. The treatment of chronic osteomyelitis with a biodegradable antibiotic-impregnated implant. *J Orthopaed Surg* 2002; 10:53–60.
24. Patzakis MJ, Mazur K, Wilkins J, Sherman R, Holtom P. Septopal beads and autogenous bone grafting for bone defects in patients with chronic osteomyelitis. *Clin Orthopaed Relat Res* 1993; 295: 112–118.
25. Itokazu M, Yamamoto K, Yang WY, Aoki T, Kato N, Watanabe K. The sustained release of antibiotic from freeze-dried fibrin-antibiotic compound and efficacies in a rat model of osteomyelitis. *Infection* 1997; 25:359–363.
26. Teixeira S, Oliveira S, Ferraz M, Monteiro F. Three dimensional macroporous calcium phosphate scaffolds for bone tissue engineering. *Key Eng Mater* 2008; 361:947–950.
27. Rose FR, Cyster LA, Grant DM, Scotchford CA, Howdle SM, Shakesheff KM. In vitro assessment of cell penetration into porous hydroxyapatite scaffolds with a central aligned channel. *Biomaterials* 2004; 25:5507–5514.
28. Karageorgiou V, Kaplan D. Porosity of 3D biomaterial scaffolds and osteogenesis. *Biomaterials* 2005; 26:5474–5491.
29. Leong MF, Chian KS, Mhaissalkar PS, Ong WF, Ratner BD. Effect of electrospun poly(d,l-lactide) fibrous scaffold with nanoporous surface on attachment of porcine esophageal epithelial cells and protein adsorption. *J Biomed Mater Res Part A* 2009; 89:1040–1048.
30. Laranjeira MS, Fernandes MH, Monteiro FJ. Response of monocultured and co-cultured human microvascular endothelial cells and mesenchymal stem cells to macroporous granules of nanostructured-hydroxyapatite agglomerates. *J Biomed Nanotechnol* 2013; 9:1594–1606.
31. Dion A, Langman M, Hall G, Filiaggi M. Vancomycin release behaviour from amorphous calcium polyphosphate matrices intended for osteomyelitis treatment. *Biomaterials* 2005; 26:7276–7285.
32. Kojima C, Watanabe K. Adsorption and desorption of bioactive proteins on hydroxyapatite for protein delivery systems. *J Drug Deliv* 2012; 2012:1–4.
33. Uquillas JA, Akkus O. Modeling the electromobility of type-I collagen molecules in the electrochemical fabrication of dense and aligned tissue constructs. *Ann Biomed Eng* 2012; 40:1641–1653.
34. Patil S, Sandberg A, Heckert E, Self W, Seal S. Protein adsorption and cellular uptake of cerium oxide nanoparticles as a function of zeta potential. *Biomaterials* 2007; 28:4600–4607.
35. Ginebra MP, Traykova T, Planell JA. Calcium phosphate cements as bone drug delivery systems: A review. *J Control Release* 2006; 113:102–110.
36. Fallgren C, Andersson A, Ljungh Å. The role of glycosaminoglycan binding of staphylococci in attachment to eukaryotic host cells. *Curr Microbiol* 2001; 43:57–63.
37. Vijan LE. The interaction of vancomycin with DNA. *Rev Roum Chim* 2009; 54:807–813.
38. Johnson JL, Yalkowsky SH. Reformulation of a new vancomycin analog: An example of the importance of buffer species and strength. *AAPS PharmSciTech* 2006; 7:E33–E37.
39. Bhateja P, Mathur T, Pandya M, Fatma T, Rattan A. Detection of vancomycin resistant *Staphylococcus aureus*: A comparative study of three different phenotypic screening methods. *Indian J Med Microbiol* 2005; 23:52.
40. Ribeiro M, Monteiro FJ, Ferraz MP. *Staphylococcus aureus* and *Staphylococcus epidermidis* adhesion to nanohydroxyapatite in the presence of model proteins. *Biomed Mater* 2012; 7: 045010.
41. Grenho L, Manso MC, Monteiro FJ, Ferraz MP. Adhesion of *Staphylococcus aureus*, *Staphylococcus epidermidis*, and *Pseudomonas aeruginosa* onto nanohydroxyapatite as a bone regeneration material. *J Biomed Mater Res Part A* 2012; 100A:1823–1830.
42. Götz F. Staphylococcus and biofilms. *Mol Microbiol* 2002; 43: 1367–1378.
43. Lew DP, Waldvogel FA. Osteomyelitis. *N Engl J Med* 1997; 336: 999–1007.
44. Pascu C, Ljungh Å, Wadström T. Staphylococci bind heparin-binding host growth factors. *Curr Microbiol* 1996; 32:201–207.